2022 American Control Conference (ACC)
Atlanta, USA, June 8-10, 2022

Adversarial Multi-agent Leader-Follower Graphical Game with Local and Global Objectives

Yusuf Kartal, Ahmet Taha Koru, Frank L. Lewis, Atilla Dogan

***Abstract*— Multiple leader and follower graphical games constitute challenging problems for aerospace and robotics applications. One of the challenges arises from having a different number of followers and leaders. We overcome this by employing an output containment error system that results in a formulation where outputs of all followers are proved to converge the convex hull spanned by the outputs of leaders. Another challenge is to design distributed Nash equilibrium control strategies for such games, which cannot be achieved with traditional quadratic cost functional formulation. Therefore, a modified cost functional that provides both Nash and distributed control strategies in the sense that each follower uses the state information of its own and neighbors, is presented. Furthermore, an $\mathcal{L}_2$ gain bound of the output containment error system that experiences unbounded disturbances is investigated by a recently developed class of digraphs that results in a semi-simple pinned graph Laplacian.**

I. Introduction

Multi-agent systems (MAS) control is one of the most widely studied phenomena in recent years, due to capability of MAS to perform certain tasks such as transportation [1], surveillance and reconnaissance [2], and target search and detection [3]. Three recognized categories of MAS control are single-leader & single-follower [4], single-leader & multi-follower [5], and multi-leader & multi-follower (MLF) [6]. For the MLF systems, one control objective is to guarantee the convergence of the output of each follower to the dynamic convex hull spanned by the outputs of leaders [6], which can be achieved by regulating the corresponding output containment error. These studies assume that followers do not have conflicts of interests. In practice, the follower group may have conflicts of interests. To address this, a well-established differential graphical game can provide a correct framework for the analysis of the MLF systems.

In the last decade, extensive efforts have been made to achieve Nash equilibrium strategies in differential graphical games [7]-[9]. In [7], the Nash equilibrium strategy was obtained with global state information. [8] proposed min-max strategies to guarantee security-level performance when the Nash solutions of graphical game Hamilton-Jacobi-Isaacs equations do not exist. [9] suggested a modified objective functional to guarantee existence of both distributed and Nash solutions by considering single-leader & multi-follower game. In practice, except from employing the graphical Nash strategies, a MAS control design requirements may include $\mathcal{L}_2$ gain boundedness, robustness against external disturbances, and output-feedback stabilizability. These design specifications are indeed local objectives of the graphical MLF game.

Therefore, the new concept of local and global objectives arise in the literature [10]. The works [6], [8], [11], [12] are indeed related to the this new concept. In [6], sufficient local conditions in terms of stabilizing the local followers dynamics and satisfying a certain $\mathcal{H}_\infty$ criterion are investigated without considering conflicts of interest between the followers. [8] analyzed the multi-agent pursuit-evasion game where pursuer group have local objective, staying together, and global objective, capturing the evaders. [10] employed local objectives for a subset of agents, on the other hand, are tasks determined around the global objective by agent-specific exosystems. Most of these works do not yield local and graphical Nash solutions simultaneously.

In this paper, we first consider a local $\mathcal{H}_\infty$ game. In this game, the control is required to minimize corresponding objective functional, whereas the disturbance is required to maximize. This corresponds to a well-known zero-sum game concept [13]. After playing the local game, we consider differential graphical game where followers' conflict of interests are addressed. Furthermore, we give sufficient conditions on the objective functional's design parameters to satisfy both of the local and global objectives simultaneously.

II. Preliminaries

This section presents various definitions on adversarial multi-agent leader-follower (MLF) games by revealing multi-agent system dynamics and communication graph topologies that are of interest.

A. Graph Topologies

A communication graph for N followers is denoted with a pair $\mathrm{G^f} = (V^f, E^f)$, where the set $V^f = \{\mathrm{v_1^f}, ..., \mathrm{v_N^f}\}$ denotes the nodes, and E^f stands for the edges, which is composed of node pairs $(\mathrm{v_i^f}, \mathrm{v_k^f})$. Each edge $\left(\mathrm{v_k^f}, \mathrm{v_i^f}\right) \in E^f$, has a weight $a_{ik}^f = 1$ if node k is connected to node i and $a_{ik}^f = 0$ otherwise. The graph is called as undirected if $a_{ik}^f = a_{ki}^f$, $\forall \mathrm{i}, \mathrm{k}$, otherwise it is termed a digraph. The in-degree matrix $\boldsymbol{D^f} = \mathrm{diag}\{d_i^f\}$ where $d_i^f = \sum_{k=1}^N a_{ik}^f$ is i^{th} row sum of adjacency matrix $\boldsymbol{\mathcal{A}^f}$. Then, the graph Laplacian matrix for the follower group is defined as $\boldsymbol{\mathcal{L}^f} = \boldsymbol{D^f} - \boldsymbol{\mathcal{A}^f}$. In this paper, we assume that $\mathrm{G^f}$ is a digraph that does not contain self loops, i.e, $a_{ii}^f = 0$.

In addition, define bipartite graph $\mathrm{G^b} = (V^f, V^l, E^b)$ that consists of follower nodes V^f, leader nodes V^l, and

Yusuf Kartal, Ahmet Taha Koru, and Frank L. Lewis are with the UTA Research Institute, Fort Worth, Texas, USA (email: yusuf.kartal@mavs.uta.edu).

Atilla Dogan is with the Aerospace Engineering Department, University of Texas at Arlington, Arlington, Texas, USA.

978-1-6654-5196-3/$31.00 ©2022 AACC

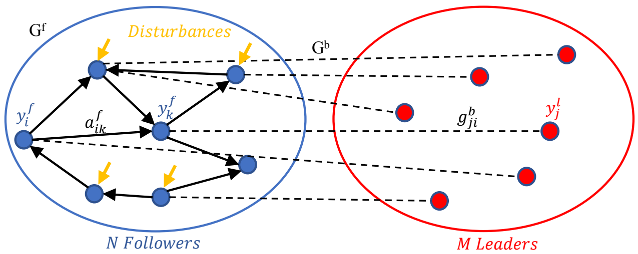

Fig. 1. Layout of Adversarial Leader-Follower Graphical Game

edges E^b, which captures the information exchange among the follower and leader groups. Let g^b_{ji} denote the pinning of follower i to leader j, with $g^b_{ji} = 1$ if follower i is connected to leader j, and $g^b_{ji} = 0$ otherwise. Additionally, let g^b_{ij} denote the pinning of leader j to follower i, with $g^b_{ij} = 1$ if leader j is pinned to follower i, and $g^b_{ij} = 0$ otherwise. Then pinning matrices of follower i and leader j in $\mathrm{G^b}$ are $\boldsymbol{G^b_j}$ and $\boldsymbol{G^b_i}$ respectively. One of the contributions of this paper is to analyze MLF games with directed communication graph topologies that lead to the limited measurement capabilities among the agents ($\mathrm{G^f}$ nodes) of game.

We use the following notations throughout this paper $\boldsymbol{I_N} \in \mathbb{R}^{N\times N}$ is the identity matrix. $\boldsymbol{1_N} \in \mathbb{R}^N$ is a vector whose elements are all one. $\mathrm{diag}(\zeta_i)$ represents a diagonal matrix with ζ_i $\forall i \in 1, ..., N$ on its diagonal. The condition $\boldsymbol{R} > 0$ (≥ 0) denotes the positive (semi) definiteness of a matrix $\boldsymbol{R}$. Kronecker product operator is denoted by $\otimes$. Lastly, distance from $\boldsymbol{x} \in \mathbb{R}^n$ to the set $\mathbb{C} \subseteq \mathbb{R}^n$ is defined via Euclidean norm as $\mathrm{dist}(\boldsymbol{x}, \mathbb{C}) = \inf_{\boldsymbol{y}\in\mathbb{C}} ||\boldsymbol{x} - \boldsymbol{y}||_2$.

B. Multi-agent System Dynamics and Local Errors

Consider the state-space representation of a follower group that consists of N dynamical agents

$$\begin{aligned} \dot{\boldsymbol{x}}^{\boldsymbol{f}}_{\boldsymbol{i}} &= \boldsymbol{A}\boldsymbol{x}^{\boldsymbol{f}}_{\boldsymbol{i}} + \boldsymbol{B}\boldsymbol{u_i} + \boldsymbol{D}\boldsymbol{w_i} \\ \boldsymbol{y}^{\boldsymbol{f}}_{\boldsymbol{i}} &= \boldsymbol{C}\boldsymbol{x}^{\boldsymbol{f}}_{\boldsymbol{i}}, \end{aligned} \tag{1}$$

$\forall i \in 1, ..., N$, where $\boldsymbol{A} \in \mathbb{R}^{n\times n}$, $\boldsymbol{B} \in \mathbb{R}^{n\times m}$, $\boldsymbol{D} \in \mathbb{R}^{n\times p}$ are system-state, input, disturbance matrices, and $\boldsymbol{C} \in \mathbb{R}^{q\times n}$ is assumed to be a full row-rank output matrix to avoid redundant measurements. The corresponding vectors $\boldsymbol{x}^{\boldsymbol{f}}_{\boldsymbol{i}}(t)$, $\boldsymbol{u_i}(t)$, $\boldsymbol{w_i}(t)$, and $\boldsymbol{y}^{\boldsymbol{f}}_{\boldsymbol{i}}(t)$ stand for the state, input, disturbance and output of i^{th} follower respectively. Additionally, consider the state-space representation of a leader group that consists of M dynamical agents

$$\begin{aligned} \dot{\boldsymbol{x}}^{\boldsymbol{l}}_{\boldsymbol{j}} &= \boldsymbol{A}\boldsymbol{x}^{\boldsymbol{l}}_{\boldsymbol{j}} \\ \boldsymbol{y}^{\boldsymbol{l}}_{\boldsymbol{j}} &= \boldsymbol{C}\boldsymbol{x}^{\boldsymbol{l}}_{\boldsymbol{j}}, \end{aligned} \tag{2}$$

$\forall j \in 1, ..., M$, where vectors $\boldsymbol{x}^{\boldsymbol{l}}_{\boldsymbol{j}}(t)$, and $\boldsymbol{y}^{\boldsymbol{l}}_{\boldsymbol{j}}(t)$ stand for the state, and output of j^{th} leader respectively.

Assumption 1: The pair $(\boldsymbol{A}, \boldsymbol{B})$ is *stabilizable*.

Assumption 2: The dynamical system (1) is output feedback (OPFB) stabilizable in the sense that the row-space of output matrix C contains the sub-space that is spanned by the right eigenvectors correspond to the unstable modes of A.

The Assumption 2 can be interpreted such that all unstable modes are measured by the output matrix C that represents the sensors installed in the systems (1).

Definition 1: A set $\mathbb{S}$ is convex if the line segment between any two points in $\mathbb{S}$ lies in $\mathbb{S}$, i.e., for any $s_1, s_2 \in \mathbb{S}$ and any $\theta \in [0, 1]$, $(\theta s_1 + (1-\theta)s_2) \in \mathbb{S}$ holds [15]. Let $Y_{G^l} = \{\boldsymbol{y^l_1}, ..., \boldsymbol{y^l_M}\}$ be the set of leaders' positions. The convex hull of a set Y_{G^l} denoted by $\mathrm{conv}(Y_{G^l})$, is the minimal convex combinations of all points in Y_{G^l} such that $\mathrm{conv}(Y_{G^l}) = \{\sum_{j=1}^M \gamma_j \boldsymbol{y^l_j} | \boldsymbol{y^l_j} \in Y_{G^l}, \gamma_j \geq 0, \sum_{j=1}^M \gamma_j = 1\}$ where the convex combination of leaders' positions $\sum_{j=1}^M \gamma_j \boldsymbol{y^l_j}$ can be reduced to the centroid of leaders' positions when $\gamma_j = 1/M, \forall j \in 1, ..., M$.

Definition 2: Consider the i^{th} follower dynamics (1) and the j^{th} leader dynamics (2), the outputs of all followers are said to converge the convex hull spanned by the outputs of leaders if

$$\lim_{t\to\infty} \mathrm{dist}(\boldsymbol{y^f_i}, \mathrm{conv}(Y_{G^l})) = 0, \forall i \in 1, ..., N. \tag{3}$$

Motivated by [6], the local relevant output containment vector for i^{th} follower is defined as

$$\begin{aligned} \boldsymbol{\xi_i} &= \sum_{i=1}^{N} a^f_{ik}(\boldsymbol{y^f_k} - \boldsymbol{y^f_i}) + \sum_{j=1}^{M} g^b_{ij}(\boldsymbol{y^f_j} - \boldsymbol{y^l_i}) \\ &= \sum_{j=1}^{M} \left(\frac{1}{M} \sum_{i=1}^{N} a^f_{ik}(\boldsymbol{y^f_k} - \boldsymbol{y^f_i}) + g^b_{ij}(\boldsymbol{y^f_j} - \boldsymbol{y^l_i}) \right). \end{aligned} \tag{4}$$

The global form of (4) is

$$\boldsymbol{\xi} = -\sum_{j=1}^{M} \Big((\boldsymbol{\psi_j} \otimes \boldsymbol{I_q})(\boldsymbol{y^f} - \underline{\boldsymbol{y}}^{\boldsymbol{l}}_{\boldsymbol{j}}) \Big) \tag{5}$$

where $\boldsymbol{\xi} = [\boldsymbol{\xi^T_1}, ..., \boldsymbol{\xi^T_N}]^T$, $\boldsymbol{\psi_j} = \frac{1}{M}\boldsymbol{\mathcal{L}^f} + \boldsymbol{G^b_j}$, $\underline{\boldsymbol{y}}^{\boldsymbol{l}}_{\boldsymbol{j}} = \boldsymbol{1_N} \otimes \boldsymbol{y^l_j}$, and $\boldsymbol{y^f} = [\boldsymbol{y^f_1}^T, ..., \boldsymbol{y^f_N}^T]^T$. Next assumption enables us to verify the output containment control objective (3) is achieved if $\lim_{t\to\infty} \boldsymbol{\xi} = \boldsymbol{0}$.

Assumption 3: Follower i in $\mathrm{G^f}$ is either a well-informed one or an uninformed one. There exists at least one well-informed follower k where $k \neq i$ $\forall k = 1, ..., N$ in $\mathrm{G^f}$ that has a directed path to uninformed follower i.

Corollary 1: Given Assumption 3, $\boldsymbol{\psi_j}$ and $\sum_{j=1}^M \boldsymbol{\psi_j}$ are non-singular M matrices, and hence the real parts of their eigenvalues are positive [6].

Remark 1: Assumption 3 implies that a unified communication graph $\mathrm{G^f} \cup \mathrm{G^b}$ has a spanning tree from each leader to each follower. This allows us to verify non-singular M-matrix property of the matrices $\boldsymbol{\psi_j}$ and $\sum_{j=1}^M \boldsymbol{\psi_j}$. Therefore, their inverses, $(\boldsymbol{\psi_j})^{-1}$ and $(\sum_{j=1}^M \boldsymbol{\psi_j})^{-1}$, exist and are non-negative. A comprehensive fifty properties of M-matrices are detailed in [14].

Lemma 1: Given the Corollary 1, consider i^{th} follower and j^{th} leader dynamics in (1) and (2). The condition (3) is achieved if $\lim_{t\to\infty} \boldsymbol{\xi} = \boldsymbol{0}$.

Proof: Re-write the global form of relevant output containment vector (5) as

$$\boldsymbol{\xi} = -\left(\sum_{j=1}^{M}(\boldsymbol{\psi_j} \otimes \boldsymbol{I_q})\right)\boldsymbol{y^f} + \sum_{j=1}^{M}\left((\boldsymbol{\psi_j} \otimes \boldsymbol{I_q})\underline{\boldsymbol{y}}_{\boldsymbol{j}}^{\boldsymbol{l}}\right) \quad (6)$$

$\lim_{t\to\infty} \boldsymbol{\xi} = \boldsymbol{0}$ implies that

$$\begin{aligned}\boldsymbol{y^f} &\to \left(\sum_{j=1}^{M}(\boldsymbol{\psi_j} \otimes \boldsymbol{I_q})\right)^{-1}\sum_{j=1}^{M}\left((\boldsymbol{\psi_j} \otimes \boldsymbol{I_q})\underline{\boldsymbol{y}}_{\boldsymbol{j}}^{\boldsymbol{l}}\right)\\ &\to \sum_{j=1}^{M}\left[\left(\sum_{r=1}^{M}(\boldsymbol{\psi_r} \otimes \boldsymbol{I_q})\right)^{-1}(\boldsymbol{\psi_j} \otimes \boldsymbol{I_q})\underline{\boldsymbol{y}}_{\boldsymbol{j}}^{\boldsymbol{l}}\right] \quad (7)\\ &\to \sum_{j=1}^{M}\left[\left(\left(\sum_{r=1}^{M}\boldsymbol{\psi_r}\right)^{-1}\boldsymbol{\psi_j}\boldsymbol{1_N}\right) \otimes \boldsymbol{y}_{\boldsymbol{j}}^{\boldsymbol{l}}\right]\end{aligned}$$

as $t \to \infty$. Realize that

$$\sum_{j=1}^{M}\left[\left(\sum_{r=1}^{M}\boldsymbol{\psi_r}\right)^{-1}\boldsymbol{\psi_j}\boldsymbol{1_N}\right] = \left(\sum_{r=1}^{M}\boldsymbol{\psi_r}\right)^{-1}\left(\sum_{j=1}^{M}\boldsymbol{\psi_j}\boldsymbol{1_N}\right) = \boldsymbol{1_N}, \quad (8)$$

which implies that each row sum of the vectors $\left(\sum_{r=1}^{M}\boldsymbol{\psi_r}\right)^{-1}\boldsymbol{\psi_j}\boldsymbol{1_N}\ \forall j \in 1,...,M$ is equal to 1. Using Corollary 1 and Remark 1, one can derive non-negative definiteness of each entry of the vectors $\left(\sum_{r=1}^{M}\boldsymbol{\psi_r}\right)^{-1}\boldsymbol{\psi_j}\boldsymbol{1_N}$ [17]. Therefore, $\lim_{t\to\infty} \boldsymbol{\xi} = \boldsymbol{0}$ indeed verifies that the condition (3) is achieved by the Definition 1. This completes the proof. □

C. Multi-agent Error Dynamics and $\mathcal{L}_2$ Gain Bound

Based on (7) in Lemma 1, define the global output containment vector as

$$\boldsymbol{\delta_y} = \boldsymbol{y^f} - \left(\sum_{j=1}^{M}(\boldsymbol{\psi_j} \otimes \boldsymbol{I_q})\right)^{-1}\sum_{j=1}^{M}\left((\boldsymbol{\psi_j} \otimes \boldsymbol{I_q})\underline{\boldsymbol{y}}_{\boldsymbol{j}}^{\boldsymbol{l}}\right). \quad (9)$$

Note that $\lim_{t\to\infty} \boldsymbol{\delta_y} = \boldsymbol{0} \implies \lim_{t\to\infty} \boldsymbol{\xi} = \boldsymbol{0}$ and (3) holds. Then, the global state containment vector is

$$\boldsymbol{\delta} = \boldsymbol{x^f} - \left(\sum_{j=1}^{M}(\boldsymbol{\psi_j} \otimes \boldsymbol{I_n})\right)^{-1}\sum_{j=1}^{M}\left((\boldsymbol{\psi_j} \otimes \boldsymbol{I_n})\underline{\boldsymbol{x}}_{\boldsymbol{j}}^{\boldsymbol{l}}\right) \quad (10)$$

where $\boldsymbol{\delta} = [\boldsymbol{\delta_1^T}, ..., \boldsymbol{\delta_N^T}]^T$, $\boldsymbol{x^f} = [\boldsymbol{x_1^f}^T, ..., \boldsymbol{x_N^f}^T]^T$ and $\underline{\boldsymbol{x}}_{\boldsymbol{j}}^{\boldsymbol{l}} = \boldsymbol{1_N} \otimes \boldsymbol{x_j^l}$.

Corollary 2: Consider global containment vectors, (9) and (10), and i^{th} follower dynamics (1) and the j^{th} leader dynamics (2). Then, by using the fact that $\boldsymbol{\xi} = -\left(\sum_{j=1}^{M}(\boldsymbol{\psi_j} \otimes \boldsymbol{I_q})\right)\boldsymbol{\delta_y}$, the output containment error system can be written in the following global form

$$\begin{aligned}\dot{\boldsymbol{\delta}} &= (\boldsymbol{I_N} \otimes \boldsymbol{A})\boldsymbol{\delta} + (\boldsymbol{I_N} \otimes \boldsymbol{B})\boldsymbol{u} + (\boldsymbol{I_N} \otimes \boldsymbol{D})\boldsymbol{w}\\ \boldsymbol{\xi} &= -\left(\sum_{j=1}^{M}(\boldsymbol{\psi_j} \otimes \boldsymbol{C})\right)\boldsymbol{\delta}.\end{aligned} \quad (11)$$

where $\boldsymbol{u} = [\boldsymbol{u_1^T}, ..., \boldsymbol{u_N^T}]^T$, and $\boldsymbol{w} = [\boldsymbol{w_1^T}, ..., \boldsymbol{w_N^T}]^T$.

Definition 3: A matrix is called as semi-simple if the geometric multiplicity of each eigenvalue is equal to its algebraic multiplicity. Further, it is diagonalizable over real set $\mathbb{R}$, if it is semi-simple and every eigenvalue is real [14].

Definition 4: Realization of the following inequality $\forall \boldsymbol{w} \in [0, \infty)$ implies that the system (11) $\mathcal{L}_2$ gain is bounded by a prescribed disturbance attenuation level denoted by γ

$$\int_0^\infty \boldsymbol{\xi^T\xi} dt \leq \gamma^2 \int_0^\infty \boldsymbol{w^T w} dt + \beta \quad (12)$$

where β is a non-negative constant. The condition (4) is also called as nonexpansivity constraint [16]. The following Lemma is inspired by [5]

Lemma 2: Given Definitions 3, 4, and output containment error system (11). Assume that $\left(\sum_{r=1}^{M}\boldsymbol{\psi_r}\right)$ is a semi-simple matrix and a stabilizing static output feedback (OPFB) control is selected as

$$\boldsymbol{u_i} = -c_i^d \boldsymbol{K_i \xi_i} \quad (13)$$

where c_i^d is a positive constant. Then, the output containment objective (3) and $\mathcal{L}_2$ gain bound condition (12) hold if the distributed N systems

$$\begin{aligned}\dot{\hat{\boldsymbol{\delta}}}_{\boldsymbol{i}} &= \boldsymbol{A}\hat{\boldsymbol{\delta}}_{\boldsymbol{i}} + \boldsymbol{B}\hat{\boldsymbol{u}}_{\boldsymbol{i}} + \boldsymbol{D}\hat{\boldsymbol{w}}_{\boldsymbol{i}}\\ &= (\boldsymbol{A} - c_i^d\lambda_i \boldsymbol{BKC})\hat{\boldsymbol{\delta}}_{\boldsymbol{i}} + \boldsymbol{D}\hat{\boldsymbol{w}}_{\boldsymbol{i}}\\ \hat{\boldsymbol{\xi}}_{\boldsymbol{i}} &= -\lambda_i \boldsymbol{C}\hat{\boldsymbol{\delta}}_{\boldsymbol{i}}\end{aligned} \quad (14)$$

are both asymptotically stable and $\mathcal{L}_2$ gain bounded by $\gamma > 0$, where λ_i are eigenvalues of the matrix $\sum_{j=1}^{M}\boldsymbol{\psi_j}$.

Proof: By Definition 3 the M-matrix $\sum_{j=1}^{M}\boldsymbol{\psi_j}$ is diagonalizable, thereby there exists an invertible transformation matrix $\boldsymbol{T}$ such that

$$\boldsymbol{T}(\sum_{j=1}^{M}\boldsymbol{\psi_j})\boldsymbol{T^{-1}} = \boldsymbol{\Lambda} = \text{diag}(\lambda_1, ..., \lambda_N). \quad (15)$$

Let $\hat{\boldsymbol{\delta}} = (\boldsymbol{T} \otimes \boldsymbol{I_n})\boldsymbol{\delta}$, $\boldsymbol{w} = (\boldsymbol{T^{-1}} \otimes \boldsymbol{I_p})\hat{\boldsymbol{w}}$, and $\hat{\boldsymbol{\xi}} = (\boldsymbol{T} \otimes \boldsymbol{I_q})\boldsymbol{\xi}$. Then (14) can be written in the global form as

$$\begin{aligned}\dot{\hat{\boldsymbol{\delta}}} &= (\boldsymbol{I_N} \otimes \boldsymbol{A} - c_i^d \boldsymbol{\Lambda} \otimes \boldsymbol{BKC})\hat{\boldsymbol{\delta}} + (\boldsymbol{I_N} \otimes \boldsymbol{D})\hat{\boldsymbol{w}}\\ \hat{\boldsymbol{\xi}} &= -(\boldsymbol{\Lambda} \otimes \boldsymbol{C})\hat{\boldsymbol{\delta}}.\end{aligned} \quad (16)$$

Realize that $\mathcal{L}_2$ norm equivalence of the pairs $(\boldsymbol{\xi}, \hat{\boldsymbol{\xi}})$ and $(\boldsymbol{w}, \hat{\boldsymbol{w}})$ are straight forward as $\boldsymbol{T}$ is invertible, and hence (11) and (16) have the same $\mathcal{L}_2$ gains. Additionally, since they have the same transfer function, the stability of equilibrium (origin) in both systems are equivalent, which completes the proof. □

III. Multi-agent Leader-Follower Game Formulation

In this section, two types of games are analyzed. The first game is a local game, which is played between control and disturbance terms of i^{th} follower. On the other hand, the second game is a global graphical game, which is played between i^{th} and j^{th} follower considering the worst case disturbance achieved in the defined local game.

Remark 2: Herein, we employ state feedback control method to derive Nash equilibrium strategies. Then, the achieved control strategies can be re-written in the OPFB form given the Assumptions 1 and 2.

A. Local $\mathcal{H}_\infty$ Game Solution

This section presents a local $\mathcal{H}_\infty$ control method, which is formulated in the form of zero-sum game by introducing the cost functional as

$$\mathcal{J}_i(\hat{\boldsymbol{u}}_i, \hat{\boldsymbol{w}}_i) = \int_t^\infty (\hat{\boldsymbol{\delta}}_i^T \boldsymbol{\mathcal{Q}}_i \hat{\boldsymbol{\delta}}_i + \frac{1}{c}\hat{\boldsymbol{u}}_i^T \boldsymbol{R}_i \hat{\boldsymbol{u}}_i - \gamma^2 \hat{\boldsymbol{w}}_i^T \hat{\boldsymbol{w}}_i) d\tau \tag{17}$$

where $\boldsymbol{\mathcal{Q}}_i \geq 0$ and $\boldsymbol{R}_i > 0$ are symmetric design matrices with appropriate dimensions. We assume that $\boldsymbol{S}_i$ is selected such that the pair $(\boldsymbol{A}, \sqrt{\boldsymbol{\mathcal{Q}}_i})$ is observable.

Now $\mathcal{H}_\infty$ control problem can be solved by treating $\hat{\boldsymbol{u}}_i$ as a minimizing player, whereas $\hat{\boldsymbol{w}}_i$ as a maximizing player of the cost (17). Then, the game can be formulated as

$$\begin{aligned}\mathcal{V}_i^*(\hat{\boldsymbol{\delta}}_i) \triangleq \mathcal{J}_i(\hat{\boldsymbol{u}}_i^*, \hat{\boldsymbol{w}}_i^*) &= \min_{\hat{\boldsymbol{u}}_i} \max_{\hat{\boldsymbol{w}}_i} \mathcal{J}_i(\hat{\boldsymbol{u}}_i, \hat{\boldsymbol{w}}_i) \\ &= \max_{\hat{\boldsymbol{w}}_i} \min_{\hat{\boldsymbol{u}}_i} \mathcal{J}_i(\hat{\boldsymbol{u}}_i, \hat{\boldsymbol{w}}_i)\end{aligned} \tag{18}$$

where $\mathcal{V}_i^*(\hat{\boldsymbol{\delta}}_i)$ and the pair $(\hat{\boldsymbol{u}}_i^*, \hat{\boldsymbol{w}}_i^*)$ denotes the optimal value functional and the local game theoretic saddle point (local Nash equilibrium) respectively.

Lemma 3: The pair $(\hat{\boldsymbol{u}}_i^*, \hat{\boldsymbol{w}}_i^*)$ constitutes a Nash equilibrium of the game (18) if

$$\hat{\boldsymbol{u}}_i^* = -c\boldsymbol{R}_i^{-1}\boldsymbol{B}^T\boldsymbol{\mathcal{P}}_i\hat{\boldsymbol{\delta}}_i, \tag{19}$$

$$\hat{\boldsymbol{w}}_i^* = \gamma^{-2}\boldsymbol{D}^T\boldsymbol{\mathcal{P}}_i\hat{\boldsymbol{\delta}}_i. \tag{20}$$

where $\boldsymbol{\mathcal{P}}_i$ is the solution of corresponding Riccati equation such that

$$\boldsymbol{\mathcal{P}}_i\boldsymbol{A} + \boldsymbol{A}^T\boldsymbol{\mathcal{P}}_i - c\boldsymbol{\mathcal{P}}_i\boldsymbol{B}\boldsymbol{R}_i^{-1}\boldsymbol{B}^T\boldsymbol{\mathcal{P}}_i + \boldsymbol{\mathcal{Q}}_i + \gamma^{-2}\boldsymbol{\mathcal{P}}_i\boldsymbol{D}\boldsymbol{D}^T\boldsymbol{\mathcal{P}}_i = \boldsymbol{0}. \tag{21}$$

Proof: Begin with deriving the Hamiltonian to solve the minimizing & maximizing extrema that satisfies the Nash condition (18) as

$$\begin{aligned}\mathcal{H}_i(\nabla\mathcal{V}_i, \hat{\boldsymbol{u}}_i, \hat{\boldsymbol{w}}_i) = \hat{\boldsymbol{\delta}}_i^T\boldsymbol{\mathcal{Q}}_i\hat{\boldsymbol{\delta}}_i + \frac{1}{c}\hat{\boldsymbol{u}}_i^T\boldsymbol{R}_i\hat{\boldsymbol{u}}_i - \gamma^2\hat{\boldsymbol{w}}_i^T\hat{\boldsymbol{w}}_i \\ + \nabla\mathcal{V}_i^T(\boldsymbol{A}\hat{\boldsymbol{\delta}}_i + \boldsymbol{B}\hat{\boldsymbol{u}}_i + \boldsymbol{D}\hat{\boldsymbol{w}}_i) = 0\end{aligned} \tag{22}$$

where $\nabla\mathcal{V}_i = \partial\mathcal{V}_i/\partial\hat{\boldsymbol{\delta}}_i$ is the co-state vector and the boundary condition is $\mathcal{V}_i(0) = 0$. Using the quadratic form $\mathcal{V}_i(\hat{\boldsymbol{\delta}}_i) = \hat{\boldsymbol{\delta}}_i^T\boldsymbol{\mathcal{P}}_i\hat{\boldsymbol{\delta}}_i$ where $\boldsymbol{\mathcal{P}}_i = \boldsymbol{\mathcal{P}}_i^T$, and applying the stationarity conditions $\partial\mathcal{H}_i(\nabla\mathcal{V}_i^*, \hat{\boldsymbol{u}}_i, \hat{\boldsymbol{w}}_i)/\partial\hat{\boldsymbol{u}}_i = \boldsymbol{0}$ and $\partial\mathcal{H}_i(\nabla\mathcal{V}_i^*, \hat{\boldsymbol{u}}_i, \hat{\boldsymbol{w}}_i)/\partial\hat{\boldsymbol{w}}_i = \boldsymbol{0}$ yields the optimal control and disturbance respectively as (19) and (20). Additionally, substituting (19) and (20) into (22) and equating resultant HJI equation to zero, i.e., $\mathcal{H}_i(\nabla\mathcal{V}_i, \hat{\boldsymbol{u}}_i^*, \hat{\boldsymbol{d}}_i^*) = 0$, gives the Riccati equation (21). To prove L_2 gain bound condition (12), first re-write the Hamiltonian (22) by completing the squares as

$$\begin{aligned}\mathcal{H}_i(\nabla\mathcal{V}_i, \hat{\boldsymbol{u}}_i, \hat{\boldsymbol{d}}_i) =& (\hat{\boldsymbol{u}}_i - \hat{\boldsymbol{u}}_i^*)^T R_i(\hat{\boldsymbol{u}}_i - \hat{\boldsymbol{u}}_i^*) \\ &- \gamma^{-2}(\hat{\boldsymbol{d}}_i - \hat{\boldsymbol{d}}_i^*)^T(\hat{\boldsymbol{d}}_i - \hat{\boldsymbol{d}}_i^*)\end{aligned} \tag{23}$$

with the boundary condition $\mathcal{V}_i(\boldsymbol{0}) = 0$. Then, the cost functional (17) can be re-expressed as

$$\begin{aligned}\mathcal{J}_i(\hat{\boldsymbol{u}}_i, \hat{\boldsymbol{w}}_i) = \int_0^\infty \Big(\frac{1}{c}(\hat{\boldsymbol{u}}_i - \hat{\boldsymbol{u}}_i^*)^T\boldsymbol{R}_i(\hat{\boldsymbol{u}}_i - \hat{\boldsymbol{u}}_i^*) \\ - \gamma^{-2}(\hat{\boldsymbol{d}}_i - \hat{\boldsymbol{d}}_i^*)^T(\hat{\boldsymbol{d}}_i - \hat{\boldsymbol{d}}_i^*)\Big)dt + \mathcal{V}_i(\hat{\boldsymbol{\delta}}_i(0)).\end{aligned} \tag{24}$$

Realize that the condition $\mathcal{J}_i(\hat{\boldsymbol{u}}_i, \hat{\boldsymbol{w}}_i) \leq \beta$ implies that the non-expansivity constraint (12) holds with $\boldsymbol{\mathcal{Q}}_i \geq \boldsymbol{C}^T\boldsymbol{C}$. Select $\beta = \mathcal{V}_i(\hat{\boldsymbol{\delta}}_i(0))$, $\hat{\boldsymbol{u}}_i = \hat{\boldsymbol{u}}_i^*$. Then, (24) reduces to

$$\begin{aligned}\mathcal{J}_i(\hat{\boldsymbol{u}}_i^*, \hat{\boldsymbol{w}}_i) = -\int_0^\infty \gamma^{-2}(\hat{\boldsymbol{d}}_i - \hat{\boldsymbol{d}}_i^*)^T(\hat{\boldsymbol{d}}_i - \hat{\boldsymbol{d}}_i^*)dt + \mathcal{V}_i(\hat{\boldsymbol{\delta}}_i(0)), \\ \leq \mathcal{V}_i(\hat{\boldsymbol{\delta}}_i(0)), \quad \forall||\hat{\boldsymbol{d}}_i||_2 \in (0, \infty).\end{aligned} \tag{25}$$

This proves that the L_2 gain bound condition (12) holds with $\beta = \mathcal{V}_i(\hat{\boldsymbol{\delta}}_i(0))$, $\hat{\boldsymbol{u}}_i = \hat{\boldsymbol{u}}_i^*$. Additionally, the value of game (18) with $\hat{\boldsymbol{u}}_i = \hat{\boldsymbol{u}}_i^*$ and $\hat{\boldsymbol{d}}_i = \hat{\boldsymbol{d}}_i^*$ is $\mathcal{V}_i(\hat{\boldsymbol{\delta}}_i(0))$ by (24). To complete the proof, notice that the form (23) indeed shows that (19) and (20) are the global optimal minimizing and maximizing extrema respectively. This indeed verifies that the pair $(\hat{\boldsymbol{u}}_i^*, \hat{\boldsymbol{w}}_i^*)$ denotes the Nash equilibrium, which completes the proof. □

Remark 3: The main purpose of introducing the local game (18) is to find the worst case disturbance for the i^{th} follower (1). Since i^{th} player is responsible for acting according to not only the worst case disturbance but also strategy of the j^{th} player, thereby $\hat{\boldsymbol{u}}_i^*$ (19) is not the finalized control strategy yet.

Corollary 3: Let the distributed N systems (14) experience the worst-case disturbance derived in (20), i.e., $\hat{\boldsymbol{w}}_i = \hat{\boldsymbol{w}}_i^*$, and introduce a new matrix $\boldsymbol{F} = \boldsymbol{A} + \gamma^{-2}\boldsymbol{D}\boldsymbol{D}^T\boldsymbol{\mathcal{P}}_i$ to facilitate the analysis. Then, the transformed local output containment error dynamics become

$$\begin{aligned}\dot{\hat{\boldsymbol{\delta}}}_i &= (\boldsymbol{A} - c\lambda_i\boldsymbol{B}\boldsymbol{K}\boldsymbol{C} + \gamma^{-2}\boldsymbol{D}\boldsymbol{D}^T\boldsymbol{\mathcal{P}}_i)\hat{\boldsymbol{\delta}}_i \\ &= \boldsymbol{F}\hat{\boldsymbol{\delta}}_i + \boldsymbol{B}\hat{\boldsymbol{u}}_i \\ \hat{\boldsymbol{\xi}}_i &= -\lambda_i\boldsymbol{C}\hat{\boldsymbol{\delta}}_i\end{aligned} \tag{26}$$

as following is the natural outcome of using transformations $\hat{\boldsymbol{\delta}} = (\boldsymbol{T} \otimes \boldsymbol{I}_n)\boldsymbol{\delta}$ and $\boldsymbol{w}^* = (\boldsymbol{T}^{-1} \otimes \boldsymbol{I}_p)\hat{\boldsymbol{w}}^*$ on (20) such that

$$\hat{\boldsymbol{w}}^* = \gamma^{-2}(\boldsymbol{I}_N \otimes \boldsymbol{D}^T\boldsymbol{\mathcal{P}}_i)\hat{\boldsymbol{\delta}}. \tag{27}$$

B. Global Graphical Game Solution

This section proposes a modified cost functional for the graphical game whose players are the nodes of $\mathrm{G^f}$. The main challenge in graphical games, is to design distributed Nash equilibrium control strategies, which cannot be achieved with traditional quadratic cost functional formulation [9]. Therefore, a modified cost functional that provides both Nash and distributed control strategies in the sense that each follower uses the state information of its own and neighbors can be defined such that

$$\begin{aligned}J_i(\hat{\boldsymbol{u}}_i, \hat{\boldsymbol{u}}_{-i}) = \\ \int_t^\infty \sum_{k=1}^N (\hat{\boldsymbol{\delta}}_{ik}^T\boldsymbol{Q}_{ik}\hat{\boldsymbol{\delta}}_{ik} + \frac{1}{c}\hat{\boldsymbol{u}}_i^T\boldsymbol{R}_i\hat{\boldsymbol{u}}_i - \frac{a_{ik}^f}{c^2}\hat{\boldsymbol{u}}_k^T\boldsymbol{R}_{ik}\hat{\boldsymbol{u}}_k)d\tau.\end{aligned} \tag{28}$$

where $\hat{\boldsymbol{\delta}}_{\boldsymbol{ik}} = [\hat{\boldsymbol{\delta}}_{\boldsymbol{i}}^{\boldsymbol{T}}, \hat{\boldsymbol{\delta}}_{\boldsymbol{k}}^{\boldsymbol{T}}]^T$, $\boldsymbol{Q_{ik}} = [\tilde{\boldsymbol{Q}}_{\boldsymbol{i}}, \tilde{\boldsymbol{Q}}_{\boldsymbol{ik}}; \tilde{\boldsymbol{Q}}_{\boldsymbol{ik}}^{\boldsymbol{T}}, \hat{\boldsymbol{Q}}_{\boldsymbol{ik}}]$, and $\hat{\boldsymbol{u}}_{\boldsymbol{-i}}$ is the set of control strategies of the k^{th} player in $\mathrm{G^f}$ where $k \neq i$. Then, the corresponding game is defined as

$$V_i^g(\hat{\boldsymbol{\delta}}_{\boldsymbol{i}}, \hat{\boldsymbol{\delta}}_{\boldsymbol{-i}}) \triangleq J_i(\hat{\boldsymbol{u}}_{\boldsymbol{i}}^{\boldsymbol{g}}, \hat{\boldsymbol{u}}_{\boldsymbol{-i}}^{\boldsymbol{g}}) \leq J_i(\hat{\boldsymbol{u}}_{\boldsymbol{i}}, \hat{\boldsymbol{u}}_{\boldsymbol{-i}}^{\boldsymbol{g}}) \tag{29}$$

where the N-tuple $\{V_1^g(\hat{\boldsymbol{\delta}}_{\boldsymbol{1}}, \hat{\boldsymbol{\delta}}_{\boldsymbol{-1}}), ..., V_N^g(\hat{\boldsymbol{\delta}}_{\boldsymbol{N}}, \hat{\boldsymbol{\delta}}_{\boldsymbol{-N}})\}$ is called as global Nash equilibrium outcome and the N-tuple $\{\hat{\boldsymbol{u}}_{\boldsymbol{1}}^{\boldsymbol{g}}, ..., \hat{\boldsymbol{u}}_{\boldsymbol{N}}^{\boldsymbol{g}}\}$ denotes the Nash equilibrium strategies of the game (29).

Corollary 4: A distributed Nash equilibrium strategy can be achieved if the functional $V_i^g(\hat{\boldsymbol{\delta}}_{\boldsymbol{i}}, \hat{\boldsymbol{\delta}}_{\boldsymbol{-i}})$ depends on the its argument $\hat{\boldsymbol{\delta}}_{\boldsymbol{i}}$ solely, i.e., $V_i^g(\hat{\boldsymbol{\delta}}_{\boldsymbol{i}}, \hat{\boldsymbol{\delta}}_{\boldsymbol{-i}}) = V_i^g(\hat{\boldsymbol{\delta}}_{\boldsymbol{i}})$.

Define a quadratic function that will play a key role in the corresponding Hamiltonian derivation such that

$$V_i(\hat{\boldsymbol{\delta}}_{\boldsymbol{i}}, \hat{\boldsymbol{\delta}}_{\boldsymbol{-i}}) \triangleq V_i(\hat{\boldsymbol{\delta}}_{\boldsymbol{i}}) = \sum_{k=1}^{N} \tilde{V}_i(\hat{\boldsymbol{\delta}}_{\boldsymbol{i}}) = N \hat{\boldsymbol{\delta}}_{\boldsymbol{i}}^{\boldsymbol{T}} \tilde{\boldsymbol{P}}_{\boldsymbol{i}} \hat{\boldsymbol{\delta}}_{\boldsymbol{i}} \tag{30}$$

Corollary 5: Given the Corollary 4, the following holds

$$\begin{aligned} \frac{\partial \tilde{V}_i^T}{\partial \hat{\boldsymbol{\delta}}_{\boldsymbol{ik}}} \dot{\hat{\boldsymbol{\delta}}}_{\boldsymbol{ik}} &= \begin{bmatrix} \frac{\partial \tilde{V}_i^T}{\partial \hat{\boldsymbol{\delta}}_{\boldsymbol{i}}} & \frac{\partial \tilde{V}_i^T}{\partial \hat{\boldsymbol{\delta}}_{\boldsymbol{k}}} \end{bmatrix}^T \begin{bmatrix} \dot{\hat{\boldsymbol{\delta}}}_{\boldsymbol{i}} \\ \dot{\hat{\boldsymbol{\delta}}}_{\boldsymbol{k}} \end{bmatrix} \\ &= \frac{\partial \tilde{V}_i^T}{\partial \hat{\boldsymbol{\delta}}_{\boldsymbol{i}}} \left(\boldsymbol{F} \hat{\boldsymbol{\delta}}_{\boldsymbol{i}} + \boldsymbol{B} \hat{\boldsymbol{u}}_{\boldsymbol{i}} \right). \end{aligned} \tag{31}$$

Theorem 1: Given the cost functional (28), local output containment error dynamics and quadratic form (30). Assume that the elements of matrix $\boldsymbol{Q_{ik}}$ satisfies

$$\tilde{\boldsymbol{Q}}_{\boldsymbol{ik}} = \boldsymbol{0}_{n \times n} \tag{32}$$

$$\hat{\boldsymbol{Q}}_{\boldsymbol{ik}} = a_{ik}^f \tilde{\boldsymbol{P}}_{\boldsymbol{k}} \boldsymbol{B} \boldsymbol{R}_{\boldsymbol{k}}^{\boldsymbol{-1}} \boldsymbol{R}_{\boldsymbol{ik}} \boldsymbol{R}_{\boldsymbol{k}}^{\boldsymbol{-1}} \boldsymbol{B}^{\boldsymbol{T}} \tilde{\boldsymbol{P}}_{\boldsymbol{k}} \tag{33}$$

where $\tilde{\boldsymbol{P}}_{\boldsymbol{i}}$ and $\tilde{\boldsymbol{P}}_{\boldsymbol{k}}$ solve the corresponding algebraic Riccati equations such that

$$\boldsymbol{F^T} \tilde{\boldsymbol{P}}_{\boldsymbol{i}} + \tilde{\boldsymbol{P}}_{\boldsymbol{i}} \boldsymbol{F} + \tilde{\boldsymbol{Q}}_{\boldsymbol{i}} - c \tilde{\boldsymbol{P}}_{\boldsymbol{i}} \boldsymbol{B} \boldsymbol{R}_{\boldsymbol{i}}^{\boldsymbol{-1}} \boldsymbol{B^T} \tilde{\boldsymbol{P}}_{\boldsymbol{i}} = \boldsymbol{0}, \tag{34}$$

$$\boldsymbol{F^T} \tilde{\boldsymbol{P}}_{\boldsymbol{k}} + \tilde{\boldsymbol{P}}_{\boldsymbol{k}} \boldsymbol{F} + \tilde{\boldsymbol{Q}}_{\boldsymbol{k}} - c \tilde{\boldsymbol{P}}_{\boldsymbol{k}} \boldsymbol{B} \boldsymbol{R}_{\boldsymbol{k}}^{\boldsymbol{-1}} \boldsymbol{B^T} \tilde{\boldsymbol{P}}_{\boldsymbol{k}} = \boldsymbol{0} \tag{35}$$

Then, the Nash equilibrium strategy for i^{th} follower in the graphical game (29) takes the following form

$$\hat{\boldsymbol{u}}_{\boldsymbol{i}}^{\boldsymbol{g}} = -c \boldsymbol{R}_{\boldsymbol{i}}^{\boldsymbol{-1}} \boldsymbol{B^T} \tilde{\boldsymbol{P}}_{\boldsymbol{i}} \hat{\boldsymbol{\delta}}_{\boldsymbol{i}} \tag{36}$$

Proof: This proof consists of two parts. The first part deals with the selection of $\boldsymbol{Q_{ik}}$ to satisfy (30) and the second part rigorously analyzes the Nash equilibrium property of minimizing controls $\hat{\boldsymbol{u}}_{\boldsymbol{i}}$ derived in the first part.

Selecting $\boldsymbol{Q_{ik}}$: Given the Corollary 5, the Hamiltonian associated with the cost functional (28) is

$$\begin{aligned} H_i(\nabla \tilde{V}_i, \hat{\boldsymbol{u}}_{\boldsymbol{i}}, \hat{\boldsymbol{u}}_{\boldsymbol{-i}}) &= \sum_{k=1}^{N} \left(\nabla \tilde{V}_i^T (\boldsymbol{F} \hat{\boldsymbol{\delta}}_{\boldsymbol{i}} + \boldsymbol{B} \hat{\boldsymbol{u}}_{\boldsymbol{i}}) \right) \\ &+ \sum_{k=1}^{N} (\hat{\boldsymbol{\delta}}_{\boldsymbol{ik}}^{\boldsymbol{T}} \boldsymbol{Q_{ik}} \hat{\boldsymbol{\delta}}_{\boldsymbol{ik}} + \frac{1}{c} \hat{\boldsymbol{u}}_{\boldsymbol{i}}^{\boldsymbol{T}} \boldsymbol{R_i} \hat{\boldsymbol{u}}_{\boldsymbol{i}} - \frac{a_{ik}^f}{c^2} \hat{\boldsymbol{u}}_{\boldsymbol{k}}^{\boldsymbol{T}} \boldsymbol{R_{ik}} \hat{\boldsymbol{u}}_{\boldsymbol{k}}) = 0 \end{aligned} \tag{37}$$

where $\nabla \tilde{V}_i = \partial \tilde{V}_i / \partial \hat{\boldsymbol{\delta}}_{\boldsymbol{i}}$ with the boundary condition $\tilde{V}_i(\boldsymbol{0}) = \boldsymbol{0}$. To find the best responses, check the stationarity condition $\partial H_i(\nabla \tilde{V}_i^g, \hat{\boldsymbol{u}}_{\boldsymbol{i}}, \hat{\boldsymbol{u}}_{\boldsymbol{-i}}) / \partial \hat{\boldsymbol{u}}_{\boldsymbol{i}} = \boldsymbol{0}$, which yields

$$\hat{\boldsymbol{u}}_{\boldsymbol{i}}^{\boldsymbol{g}} = -\frac{c}{2} \boldsymbol{R}_{\boldsymbol{i}}^{\boldsymbol{-1}} \boldsymbol{B^T} \nabla \tilde{V}_i^g \tag{38}$$

Substituting (38) into (37) yields the Hamilton-Jacobi (HJ) equation, i.e., $H_i(\nabla \tilde{V}_i^g, \hat{\boldsymbol{u}}_{\boldsymbol{i}}^{\boldsymbol{g}}, \hat{\boldsymbol{u}}_{\boldsymbol{-i}}^{\boldsymbol{g}}) = 0$. Additionally, using the quadratic form of $\tilde{V}_i(\hat{\boldsymbol{\delta}}_{\boldsymbol{i}})$ (30) in the HJ equation, one obtains

$$\begin{aligned} &H_i(\nabla \tilde{V}_i^g, \hat{\boldsymbol{u}}_{\boldsymbol{i}}^{\boldsymbol{g}}, \hat{\boldsymbol{u}}_{\boldsymbol{-i}}^{\boldsymbol{g}}) = \\ &\textstyle\sum_{k=1}^{N} \hat{\boldsymbol{\delta}}_{\boldsymbol{i}}^{\boldsymbol{T}} (\boldsymbol{F^T} \tilde{\boldsymbol{P}}_{\boldsymbol{i}} + \tilde{\boldsymbol{P}}_{\boldsymbol{i}} \boldsymbol{F} + \tilde{\boldsymbol{Q}}_{\boldsymbol{i}} - c \tilde{\boldsymbol{P}}_{\boldsymbol{i}} \boldsymbol{B} \boldsymbol{R}_{\boldsymbol{i}}^{\boldsymbol{-1}} \boldsymbol{B^T} \tilde{\boldsymbol{P}}_{\boldsymbol{i}}) \hat{\boldsymbol{\delta}}_{\boldsymbol{k}} \\ &+ \textstyle\sum_{k=1}^{N} \hat{\boldsymbol{\delta}}_{\boldsymbol{k}}^{\boldsymbol{T}} (\hat{\boldsymbol{Q}}_{\boldsymbol{ik}} - a_{ik}^f \tilde{\boldsymbol{P}}_{\boldsymbol{k}} \boldsymbol{B} \boldsymbol{R}_{\boldsymbol{k}}^{\boldsymbol{-1}} \boldsymbol{R_{ik}} \boldsymbol{R}_{\boldsymbol{k}}^{\boldsymbol{-1}} \boldsymbol{B^T} \tilde{\boldsymbol{P}}_{\boldsymbol{k}}) \hat{\boldsymbol{\delta}}_{\boldsymbol{k}} = 0. \end{aligned} \tag{39}$$

This gives the elements of matrix $\boldsymbol{Q_{ik}}$ (32)-(33), and the Riccati equations (34)-(35) and completes the first part of the proof. □

Graphical Nash Equilibrium: In this part, we prove the N-tuple $\{\hat{\boldsymbol{u}}_{\boldsymbol{1}}^{\boldsymbol{g}}, ..., \hat{\boldsymbol{u}}_{\boldsymbol{N}}^{\boldsymbol{g}}\}$ indeed constitutes the Nash equilibrium strategies of the game (29). Realize that substituting the quadratic form (30) into (38) yields (36).

Now re-write the Hamiltonian (37) as

$$H_i(\nabla \tilde{V}_i, \hat{\boldsymbol{u}}_{\boldsymbol{i}}, \hat{\boldsymbol{u}}_{\boldsymbol{-i}}) = \sum_{k=1}^{N} H_{ik}(\nabla \tilde{V}_i, \hat{\boldsymbol{u}}_{\boldsymbol{i}}, \hat{\boldsymbol{u}}_{\boldsymbol{-i}}) \tag{40}$$

where $H_{ik}(\nabla \tilde{V}_i, \hat{\boldsymbol{u}}_{\boldsymbol{i}}, \hat{\boldsymbol{u}}_{\boldsymbol{-i}})$ can be expressed by completing the squares as

$$\begin{aligned} &H_{ik}(\nabla \tilde{V}_i, \hat{\boldsymbol{u}}_{\boldsymbol{i}}, \hat{\boldsymbol{u}}_{\boldsymbol{-i}}) = H_{ik}(\nabla \tilde{V}_i, \hat{\boldsymbol{u}}_{\boldsymbol{i}}^{\boldsymbol{g}}, \hat{\boldsymbol{u}}_{\boldsymbol{-i}}^{\boldsymbol{g}}) \\ &+ \frac{1}{c} (\hat{\boldsymbol{u}}_{\boldsymbol{i}} - \hat{\boldsymbol{u}}_{\boldsymbol{i}}^{\boldsymbol{g}})^T \boldsymbol{R_i} (\hat{\boldsymbol{u}}_{\boldsymbol{i}} - \hat{\boldsymbol{u}}_{\boldsymbol{i}}^{\boldsymbol{g}}) - \frac{a_{ik}^f}{c^2} (\hat{\boldsymbol{u}}_{\boldsymbol{k}} - \hat{\boldsymbol{u}}_{\boldsymbol{k}}^{\boldsymbol{g}})^T \boldsymbol{R_{ik}} (\hat{\boldsymbol{u}}_{\boldsymbol{k}} - \hat{\boldsymbol{u}}_{\boldsymbol{k}}^{\boldsymbol{g}}) \\ &- \frac{2 a_{ik}^f}{c^2} \hat{\boldsymbol{u}}_{\boldsymbol{k}}^{\boldsymbol{g}\,T} \boldsymbol{R_{ik}} (\hat{\boldsymbol{u}}_{\boldsymbol{k}} - \hat{\boldsymbol{u}}_{\boldsymbol{k}}^{\boldsymbol{g}}) \end{aligned} \tag{41}$$

since the equality $\nabla \tilde{V}_i^T \boldsymbol{B} \boldsymbol{u}_{\boldsymbol{i}}^{\boldsymbol{g}} = -\frac{2}{c} (\hat{\boldsymbol{u}}_{\boldsymbol{i}}^{\boldsymbol{g}})^T \boldsymbol{R_i} \hat{\boldsymbol{u}}_{\boldsymbol{i}}^{\boldsymbol{g}}$ holds by (38). Having the fact that Hamiltonian (37) is the differential equivalent of the cost functional (28), we can write

$$J_i(\hat{\boldsymbol{u}}_{\boldsymbol{i}}, \hat{\boldsymbol{u}}_{\boldsymbol{-i}}) = \int_{t_0}^{\infty} \sum_{k=1}^{N} H_{ik}(\nabla \tilde{V}_i, \hat{\boldsymbol{u}}_{\boldsymbol{i}}, \hat{\boldsymbol{u}}_{\boldsymbol{-i}}) dt + V_i(\hat{\boldsymbol{\delta}}_{\boldsymbol{i}}(t_0)). \tag{42}$$

According to rules of the game (29), select $\hat{\boldsymbol{u}}_{\boldsymbol{k}} = \hat{\boldsymbol{u}}_{\boldsymbol{k}}^{\boldsymbol{g}}$ and use the Hamiltonian form (41) in (42) to obtain

$$\begin{aligned} &J_i(\hat{\boldsymbol{u}}_{\boldsymbol{i}}, \hat{\boldsymbol{u}}_{\boldsymbol{-i}}^{\boldsymbol{g}}) \\ &= \int_{t_0}^{\infty} \sum_{k=1}^{N} \frac{1}{c} (\hat{\boldsymbol{u}}_{\boldsymbol{i}} - \hat{\boldsymbol{u}}_{\boldsymbol{i}}^{\boldsymbol{g}})^T \boldsymbol{R_i} (\hat{\boldsymbol{u}}_{\boldsymbol{i}} - \hat{\boldsymbol{u}}_{\boldsymbol{i}}^{\boldsymbol{g}}) dt + V_i(\hat{\boldsymbol{\delta}}_{\boldsymbol{i}}(t_0)), \end{aligned} \tag{43}$$

which clearly satisfies the game condition $J_i(\hat{\boldsymbol{u}}_{\boldsymbol{i}}^{\boldsymbol{g}}, \hat{\boldsymbol{u}}_{\boldsymbol{-i}}^{\boldsymbol{g}}) \leq J_i(\hat{\boldsymbol{u}}_{\boldsymbol{i}}, \hat{\boldsymbol{u}}_{\boldsymbol{-i}}^{\boldsymbol{g}})$, and hence the N-tuple $\{\hat{\boldsymbol{u}}_{\boldsymbol{1}}^{\boldsymbol{g}}, ..., \hat{\boldsymbol{u}}_{\boldsymbol{N}}^{\boldsymbol{g}}\}$ is indeed the Nash equilibrium of the game (29). This completes the second part of the proof. □

Remark 4: Realize that the local $\mathcal{H}_\infty$ Nash control strategy $\hat{\boldsymbol{u}}_{\boldsymbol{i}}^{\boldsymbol{*}}$ (19) has not the same form as the global graphical Nash control $\hat{\boldsymbol{u}}_{\boldsymbol{i}}^{\boldsymbol{g}}$ (36). Therefore, we have not obtained a control strategy that belongs to Nash equilibrium for both game (18) and (29). The next Theorem 2 gives necessary conditions to provide dual Nash control strategy by selecting appropriate $\tilde{\boldsymbol{Q}}_{\boldsymbol{i}}$ and $\boldsymbol{R_{ik}}$ design matrices.

Theorem 2: The Nash equilibrium control strategy $\hat{\boldsymbol{u}}_i^*$ (19) for the local $\mathcal{H}_\infty$ game (18) stands for the same Nash equilibrium control strategy $\hat{\boldsymbol{u}}_i^g$ (36) for the global graphical game (29) if the constant in (13) satisfies $c_i^d = c/\lambda_i$, and the design matrices $\tilde{\boldsymbol{Q}}_i$ and $\boldsymbol{R}_{ik}$ are selected as

$$\tilde{\boldsymbol{Q}}_i = -\gamma^{-2}\boldsymbol{\mathcal{P}}_i\boldsymbol{D}\boldsymbol{D}^T\boldsymbol{\mathcal{P}}_i + \boldsymbol{\mathcal{Q}}_i \tag{44}$$

$$\boldsymbol{R}_{ik} = N^2\boldsymbol{B}^T\boldsymbol{\mathcal{P}}_i\tilde{\boldsymbol{Q}}_i\boldsymbol{\mathcal{P}}_i\boldsymbol{B} + \tilde{\boldsymbol{R}}_{ik} \tag{45}$$

where $\tilde{\boldsymbol{R}}_{ik} > 0$.

Proof: Note that both (19) and (36) are function of constant c. Since they are written in the transformed coordinate system, their actual forms is a function of c/λ_i. Thence, the applied control's (13) constant c_i^d should be equal to c/λ_i to bring them in the same form. Now, we work on selection of the design matrix $\tilde{\boldsymbol{Q}}_i$. Begin with expanding the Riccati equation (34) using $\boldsymbol{F} = \boldsymbol{A} + \gamma^{-2}\boldsymbol{D}\boldsymbol{D}^T\boldsymbol{\mathcal{P}}_i$, which yields

$$\begin{aligned}\tilde{\boldsymbol{P}}_i\boldsymbol{A} + \boldsymbol{A}^T\tilde{\boldsymbol{P}}_i - c\tilde{\boldsymbol{P}}_i\boldsymbol{B}\boldsymbol{R}_i^{-1}\boldsymbol{B}^T\tilde{\boldsymbol{P}}_i + \tilde{\boldsymbol{Q}}_i \\ + \gamma^{-2}(\tilde{\boldsymbol{P}}_i\boldsymbol{D}\boldsymbol{D}^T\boldsymbol{\mathcal{P}}_i + \boldsymbol{\mathcal{P}}_i\boldsymbol{D}\boldsymbol{D}^T\tilde{\boldsymbol{P}}_i) = \boldsymbol{0}.\end{aligned} \tag{46}$$

Select $\tilde{\boldsymbol{Q}}_i$ as in (44), and assume that $c\boldsymbol{B}\boldsymbol{R}_i^{-1}\boldsymbol{B}^T \geq \gamma^{-2}\boldsymbol{D}\boldsymbol{D}^T$ holds. Assume that the positive definite matrix $\boldsymbol{\mathcal{P}}_i$ solves the local $\mathcal{H}_\infty$ game Riccati equation (21). Then, to verify it also solves the Graphical game Riccati equation (46), we need to show $\tilde{\boldsymbol{P}}_i = \boldsymbol{\mathcal{P}}_i$ is a positive definite solution of the Graphical Riccati equation (46), which is illustrated in the following realization

$$\begin{aligned}(\tilde{\boldsymbol{P}}_i - \boldsymbol{\mathcal{P}}_i)\boldsymbol{D}\boldsymbol{D}^T(\tilde{\boldsymbol{P}}_i - \boldsymbol{\mathcal{P}}_i) = \tilde{\boldsymbol{P}}_i\boldsymbol{D}\boldsymbol{D}^T\tilde{\boldsymbol{P}}_i + \boldsymbol{\mathcal{P}}_i\boldsymbol{D}\boldsymbol{D}^T\boldsymbol{\mathcal{P}}_i \\ - \tilde{\boldsymbol{P}}_i\boldsymbol{D}\boldsymbol{D}^T\boldsymbol{\mathcal{P}}_i - \boldsymbol{\mathcal{P}}_i\boldsymbol{D}\boldsymbol{D}^T\tilde{\boldsymbol{P}}_i,\end{aligned} \tag{47}$$

thereby (46) can be expressed in terms of $\tilde{\boldsymbol{P}}_i$ with selected $\tilde{\boldsymbol{Q}}_i$ (44) as

$$\tilde{\boldsymbol{P}}_i\boldsymbol{A} + \boldsymbol{A}^T\tilde{\boldsymbol{P}}_i - c\tilde{\boldsymbol{P}}_i\boldsymbol{B}\boldsymbol{R}_i^{-1}\boldsymbol{B}^T\tilde{\boldsymbol{P}}_i + \boldsymbol{\mathcal{Q}}_i + \gamma^{-2}\tilde{\boldsymbol{P}}_i\boldsymbol{D}\boldsymbol{D}^T\tilde{\boldsymbol{P}}_i = \boldsymbol{0}. \tag{48}$$

Realize that (48) has a dual form of (21). Therefore, the Nash equilibrium control strategies, i.e. $\hat{\boldsymbol{u}}_i^*$ (19), and $\hat{\boldsymbol{u}}_i^g$ (36), are the same as each other since the Riccati equation (21) is assumed to have a unique positive definite under some conditions, which will be illustrated in a future work.

To complete the proof, we need to show that $\boldsymbol{Q}_{ik}$ in (28) is at least positive semi-definite with the selected design matrices (32)-(33) and (44)-(45). This can be achieved if the inequality $\hat{\boldsymbol{Q}}_{ik} - \tilde{\boldsymbol{Q}}_{ik}^T\tilde{\boldsymbol{Q}}_i^{-1}\tilde{\boldsymbol{Q}}_{ik} \geq \boldsymbol{0}$ holds by using the Schur complement method. To check, substitute the selected design matrices (32)-(33) and (44)-(45) into expression $\hat{\boldsymbol{Q}}_{ik} - \tilde{\boldsymbol{Q}}_{ik}^T\tilde{\boldsymbol{Q}}_i^{-1}\tilde{\boldsymbol{Q}}_{ik}$, which yields

$$\hat{\boldsymbol{Q}}_{ik} - \tilde{\boldsymbol{Q}}_{ik}^T\tilde{\boldsymbol{Q}}_i^{-1}\tilde{\boldsymbol{Q}}_{ik} = a_{ik}^f\tilde{\boldsymbol{P}}_k\boldsymbol{B}\boldsymbol{R}_k^{-1}\tilde{\boldsymbol{R}}_{ik}\boldsymbol{R}_k^{-1}\boldsymbol{B}^T\tilde{\boldsymbol{P}}_k \geq \boldsymbol{0}. \tag{49}$$

This completes the proof. □

Remark 5: The Theorem 2 implies that i^{th} player can minimize its global cost (28) by only playing the local $\mathcal{H}_\infty$ (18) game. Thence, if the i^{th} player stabilizes the local error dynamics (14) with the Nash equilibrium control strategy (19), then both of the local and global objectives can be satisfied simultaneously.

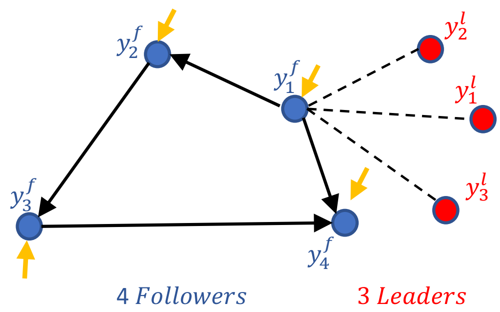

Fig. 2. The communication graph of the four followers and three leaders MLF game.

IV. Multi-agent Leader-Follower Game Simulation

This section presents a numerical example to verify the proposed methods. Consider the double integrator dynamics driven by different types of actuators [18] whose system matrices for the follower (1) and the leader (2) groups are given as

$$\begin{aligned}\boldsymbol{A} = \begin{bmatrix}0 & 1 & 0\\ 0 & 0 & 2\\ 0 & -3 & -2\end{bmatrix}; \boldsymbol{B} = \begin{bmatrix}0 & 0 & 2\end{bmatrix}^T; \\ \boldsymbol{C} = \begin{bmatrix}1 & 0 & 0\end{bmatrix}; \boldsymbol{D} = \begin{bmatrix}0 & 0 & 1\end{bmatrix}^T.\end{aligned} \tag{50}$$

The adjacency matrix $\boldsymbol{\mathcal{A}^f}$ that connects $N = 4$ followers or nodes of the graph $\mathrm{G^f}$ and the bipartite communication graph parameters $\boldsymbol{G_j^b}$ $j \in \{1, ..., M = 3\}$ that do not contradict with Assumption 3 are selected as

$$\boldsymbol{\mathcal{A}^f} = \begin{bmatrix}0 & 0 & 0 & 0\\ 1 & 0 & 0 & 0\\ 0 & 1 & 0 & 0\\ 1 & 0 & 1 & 0\end{bmatrix}, \; g_{11}^b = g_{12}^b = g_{13}^b = 1. \tag{51}$$

The MLF game communication graph is illustrated in Fig. 2. Note that the root node is selected as the first follower $\boldsymbol{y_1^f}$ according to the Assumption 3. There is also no connection from uninformed followers $(\boldsymbol{y_2^f}, \boldsymbol{y_3^f}, \boldsymbol{y_4^f})$ to the well informed follower $\boldsymbol{y_1^f}$ and the follower graph is an acyclic digraph. The eigenvalues of the pinned Laplacian matrix $(\sum_{j=1}^M \boldsymbol{\psi_j})$ are $3.000, 0.667, 0.333, 0.333$. Further, we select the coupling gain $c = 1$ and hence $c_1^d = 0.333$, $c_2^d = 1.5$, and $c_3^d = c_4^d = 3$ as given in Theorem 2. Lastly, the attenuation level set to $\gamma = 3$, and the disturbance is evaluated using (20).

The resultant gains of follower group in (13) are derived using the Riccati equation solutions (34) and (35) as

$$\begin{aligned}\boldsymbol{K_1} &= \begin{bmatrix}1.3432 & 1.1630 & 1.2649\end{bmatrix};\\ \boldsymbol{K_2} &= \begin{bmatrix}0.6358 & 0.3946 & 0.48049\end{bmatrix};\\ \boldsymbol{K_3} = \boldsymbol{K_4} &= \begin{bmatrix}0.4519 & 0.2422 & 0.2986\end{bmatrix}.\end{aligned} \tag{52}$$

In simulations, we assume that the initial states of followers and leaders are uniformly distributed in the interval $[0, 1]$. Then, the MLF game is started by applying the control

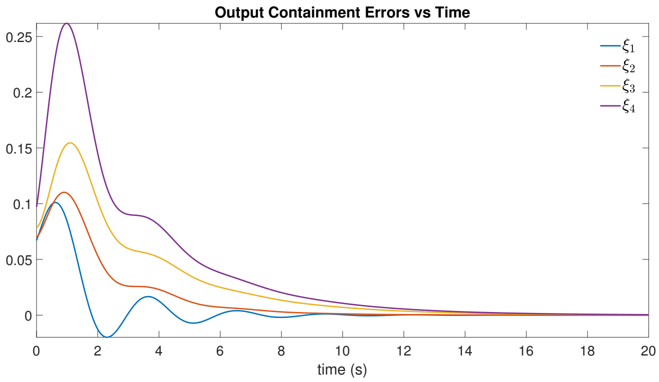

Fig. 3. Convergence of output containment errors.

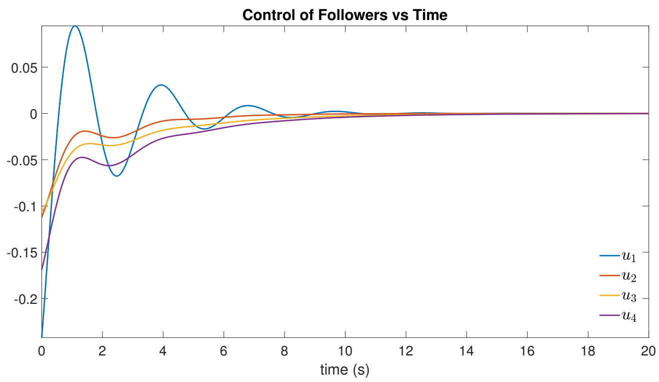

Fig. 4. Control trajectories of followers.

strategies (13). Notice that the communication graph of the four followers and three leaders MLF game is illustrated in Fig. 2. Fig. 3 shows the convergence of the output containment errors (4) to zero. The global form of containment vector is derived by using (5). Fig. 4 illustrates the control trajectories (13) of each follower. These indeed verify the correct performance of the proposed methods.

V. Summary and Future Work

In this paper, we proposed a novel local and global objectives for the MLF output containment game for the LTI multi-agent systems. The local $\mathcal{H}_\infty$ game is solved for the Nash equilibrium strategies where controls are minimizing and disturbances are maximizing players. On the other hand, the graphical game is introduced as a global objective to address mutual interests among the followers. However, stability and robustness analysis have not been conducted. These issues will addressed in a future work. Lastly, the proposed control scheme indeed has an immense relationship with the output containment games of unmanned vehicles that include n-rotor systems. Thence, the proposed methods can be extended to apply multiple unmanned vehicle systems in a future work.

Acknowledgment

This work was Supported by NSF Grant ECCS-1839804, ARO Grant W911NF-20-1-0132, and ONR Grant N00014-18-1-2221. Author Dr. Kartal thanks Turkish Aerospace for the financial support.

References

[1] Mellinger, D., Shomin, M., Michael, N., Kumar, V.: 'Cooperative grasping and transport using multiple quadrotors', *Distributed Autonomous Robotic Systems*, 2013, Springer, Berlin, Heidelberg, pp. 545-558

[2] Kopfstedt, T., Mukai, M., Fujita, M., Ament, C.: 'Control of formations of UAVs for surveillance and reconnaissance missions', *IFAC Proceedings Volumes*, 2008, **41**, (2), pp. 5161-5166

[3] Waharte, S., Trigoni, N., Julier, S.: 'Coordinated search with a swarm of UAVs', *IEEE Annual Communications Society Conference on Sensor, Mesh and Ad Hoc Communications and Networks Workshops*, June 2009, pp. 1-3

[4] Kartal, Y., Subbarao, K., Dogan, A., Lewis, F.: 'Optimal game theoretic solution of the pursuitevasion intercept problem using on-policy reinforcement learning', *International Journal of Robust and Nonlinear Control*, 2021, **31**, (16), pp. 7886-7903.

[5] Jiao, Q., Modares, H., Lewis, F. L., Xu, S., Xie, L.: 'Distributed L2-gain output-feedback control of homogeneous and heterogeneous systems', 2016 *Automatica*, **71**, pp. 361-368.

[6] Zuo, S., Song, Y., Lewis, F. L., Davoudi, A.: 'Output containment control of linear heterogeneous multi-agent systems using internal model principle', *IEEE Transactions on Cybernetics*, 2017, **47**, (8), pp. 2099-2109.

[7] Vamvoudakis, K. G., Lewis, F. L., Hudas, G. R.: 'Multi-agent differential graphical games: Online adaptive learning solution for synchronization with optimality', *Automatica*, 2012, **48**, (8), pp. 1598-1611.

[8] Lopez, V. G., Lewis, F. L., Wan, Y., Sanchez, E. N., Fan, L.: 'Solutions for multiagent pursuit-evasion games on communication graphs: Finite-time capture and asymptotic behaviors', *IEEE Transactions on Automatic Control*, 2019, textbf65, (5), pp. 1911-1923.

[9] Liu, M., Wan, Y., Lopez, V. G., Lewis, F. L., Hewer, G., Estabridis, K.: 'Differential Graphical Game with Distributed Global Nash Solution', *IEEE Transactions on Control of Network Systems*, 2021, **8**, (3), pp. 1371-1382.

[10] Sarslmaz, S. B., Yucelen, T.: 'Distributed control of linear multiagent systems with global and local objectives', *Systems & Control Letters*, 2021, Early view.

[11] Chen, C., Lewis, F. L., Xie, S., Modares, H., Liu, Z., Zuo, S., Davoudi, A.: 'Resilient adaptive and H-infinity controls of multi-agent systems under sensor and actuator faults', *Automatica*, 2019, **102**, pp. 19-26.

[12] Zuo, S., Lewis, F. L., Davoudi, A.: 'Resilient output containment of heterogeneous cooperative and adversarial multigroup systems', *IEEE Transactions on Automatic Control*, 2019, **65**, (7), pp. 3104-3111.

[13] Basar, T., Bernhard, P.: 'H-infinity optimal control and related minimax design problems: a dynamic game approach', Springer Science & Business Media, 2008.

[14] Berman, A., Plemmons, R. J.: 'Nonnegative matrices in the mathematical sciences', Society for Industrial and Applied Mathematics, 1994.

[15] Boyd, S., Boyd, S. P., Vandenberghe, L.: 'Convex optimization. Cambridge University Press', 2004.

[16] Haddad, W. M., Chellaboina, V.: 'Nonlinear dynamical systems and control', Princeton university press, 2011.

[17] Dong, X., Hu, G.: 'Time-varying formation tracking for linear multiagent systems with multiple leaders', *IEEE Transactions on Automatic Control*, 2017, **62**, (7), pp. 3658-3664.

[18] Wieland, P., Sepulchre, R., Allgöwer, F.: 'An internal model principle is necessary and sufficient for linear output synchronization', *Automatica*, 2011, **47**, (5), pp. 1068-1074.